University of Groningen

Light-Controlled Conductance Using Molecular Switches

Kudernác, Tibor

IMPORTANT NOTE: You are advised to consult the publisher's version (publisher's PDF) if you wish to cite from it. Please check the document version below.

Document Version
Publisher's PDF, also known as Version of record

Publication date:
2007

Link to publication in University of Groningen/UMCG research database

Citation for published version (APA):
Kudernác, T. (2007). *Light-Controlled Conductance Using Molecular Switches*. [Thesis fully internal (DIV), University of Groningen]. s.n.

Copyright
Other than for strictly personal use, it is not permitted to download or to forward/distribute the text or part of it without the consent of the author(s) and/or copyright holder(s), unless the work is under an open content license (like Creative Commons).

The publication may also be distributed here under the terms of Article 25fa of the Dutch Copyright Act, indicated by the "Taverne" license. More information can be found on the University of Groningen website: https://www.rug.nl/library/open-access/self-archiving-pure/taverne-amendment.

Take-down policy
If you believe that this document breaches copyright please contact us providing details, and we will remove access to the work immediately and investigate your claim.

Downloaded from the University of Groningen/UMCG research database (Pure): http://www.rug.nl/research/portal. For technical reasons the number of authors shown on this cover page is limited to 10 maximum.

Download date: 07-10-2024

Chapter 2

One –Way Conductance Switching of Single Photochromic Molecules connected to Gold Electrodes

In this chapter the light-induced conductance switching of single photochromic molecules connected to gold electrodes is described. Photochromic properties of two newly synthesized diarylethenes have been studied in solution showing reversible behavior. Two experimental techniques, namely, the Mechanically Controllable Break-Junction technique and Scanning Tunneling Microscopy are used to investigate electrical properties of the open and closed states of the molecules. Switching from a conductive to an insulating state is observed upon illumination with visible light. However, upon illumination with UV light the reverse process is not observed for molecules covalently attached to gold electrodes. We have attributed this to quenching of the excited state of the molecules in the open form by the presence of metallic gold. Additionally, reversible and irreversible stochastic switching, independent of the use of light, is observed in Scanning Tunneling Microscopy experiments showing dependence on the used bias voltage.[*]

[*] Part of this chapter has been published: D. Dulic, S. J. van der Molen, T. Kudernac, H. T. Jonkman, J. J. D. de Jong, T. N. Bowden, J. van Esch, B. L. Feringa, B. J. van Wees, *Phys. Rev. Lett*. **2003**, *91*, 207402; S. J. van der Molen, H. van der Vegte, T. Kudernac, I. Amin, B. L. Feringa, B. J. van Wees, *Nanotechnology* **2006**, *17*, 310.

2.1 Introduction

A major challenge of molecular electronics is to design useful devices based on addressable molecular structures and to incorporate these into integrated circuits[1]. As a result of decades of research in this area substitutes for conventional switches,[2] rectifiers,[3] wires[4] and transistors[5] have been introduced, although still considerable effort is needed to realize practical and robust molecular based electronic devices.[6] The necessity to respond to external stimuli places molecular switches amongst the most challenging of systems.[7] Photochromic molecular switches[7] meet this requirement and specifically 1,2-dithienylethenes (Figure 1) hold a prominent position among others because of their reversible photo-induced transformations that modulate electrical conductivity and their exceptional thermal stability and fatigue resistance.[8] Despite the noticeable progress in designing new molecular electronic components, including molecular switches, their incorporation into integrated circuits remains a challenge. A common approach is based on anchoring molecules to metal electrodes.[3,9] However, in the case of photochromic molecules, the situation is more complicated, since the presence of a metal surface may influence optical processes in photoactive molecules.[10]

Another important question, which has to be addressed, is the nature of electron transport through these hybrid metal-molecular systems. Investigation of the electron transport properties of a single or a limited number of molecules connected to metallic electrodes is therefore presently the subject of intense research activity. Besides the fundamental interest in electron transport phenomena operating at the nanoscale, it also represents an important milestone for the development of molecular electronics. Part of the problem lies in the fact that if we want to perform reliable electronic transport measurements on a molecular system, we have to make a well controlled electrical contact between the molecule and the nanometer-scale electrodes used in the measurements. This connection can influence intrinsic properties of the molecules. Several techniques have been recently employed to explore conductive properties of individual or small numbers of molecules chemically connected to one or two electrodes. All the techniques involve at least one electrode of nanometer size. Mechanically Controlled Break-Junction (MCBJ),[9,11] electromigration-induced tunnel devices,[12] Scanning Tunneling Microscopy (STM)[13] or conductive-probe Atomic Force Microscopy (cAFM)[14] are all techniques measuring one or at most a few molecules. For MCBJ and electromigration, molecules are chemically connected to two electrodes, which are freshly formed in a controlled manner. In the case of MCBJ, a thin metallic wire is mechanically stretched until it breaks into two nano-dimensional electrodes. Electromigration-induced nanogaps are produced by applying large current

densities to gold wires. At high current densities j (typically 108 A/cm^2) momentum transfer from the electrons to the gold atoms leads to drift of the atoms, in the direction of the electron flow. This mass flux can lead to the growth of voids in the wire, finally leading to the formation of gaps.[15] Typical STM and cAFM setups are used to study conductance of molecules that are incorporated into a self-assembled monolayer (SAM) formed on a planar substrate. Molecules are covalently linked to a planar substrate, serving as one electrode and a conductive atomically sharp tip, positioned on top of SAMs, acts as a second electrode while scanning. In addition to the aforementioned techniques, which focus primarily on single molecules, there are other experimental setups that involve greater but nevertheless small number of molecules that are inserted between two nanometer size contact electrodes. The tunneling junction, here consisting of two metal plates separated by molecules, can be assembled using several approaches, among them: crossed wires,[16] mercury-drop junction[17] and metal-capped nanopores with[18] or without[19] a conducting polymer interlayer between the SAM and the metal top electrode to prevent formation of electrical short circuits.

The main goal of our work was to study and control the conductive properties of diarylethene photochromic molecular switches connected to metallic electrodes. Figure 1 shows a schematic of the incorporation of thiol terminated diarylethene switch between two

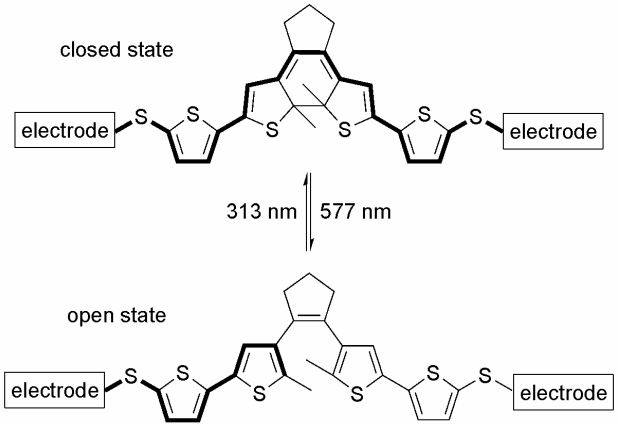

Figure 1 *A photochromic molecular switch between two electrode contacts in the closed state and the open state. By exposing the molecule to light of wavelength 577 nm, the molecule will switch from the closed to open form. The molecule can be switched back to the closed state by exposing it to UV light at 313 nm.*

electrodes. The molecule consists of conducting conjugated units, separated by switching units, which allow electron transport to be turned on-and-off reversibly by exposure to light

with specific frequencies. DFT calculations predict that the energies of diarylethene's LUMO and HOMO levels are in the range of 1.0 – 3.0 eV and 4.5 – 6.0 eV respectively.[†] In order to study the electronic transport through individual switches directly we attach them to metallic electrodes with controlled spacing in the nanometer range. In order to obtain complementary information we use two different experimental techniques: MCBJ and STM.

2.2 Synthesis and Photochromic Properties of Novel Thiol Terminated Diarylethene Compounds

Diarylethene photochromic switches **3** (Scheme 1) and **6** (Scheme 2) have been designed specifically for our electronic transport experiments. They consist of a central switching unit, two thiophene rings on both sides of the switching unit, and one (in case of **6**) or two (in case of **3**) thiol groups, protected with acetyl groups, at the ends of the molecules. The synthetic strategy has been based on Suzuki couplings and a subsequent introduction of thiol groups (Scheme 1 and 2). Compound **1** is known to be easily accessible and suitable for further functionalizations.[20] Its treatment with *n*-butyl lithium followed by tri-*n*-butyl borate gives a reactive boronic acid intermediate, which can react with a heteroaromatic bromide leading to compounds **2** or **4**. In case of **4**, subsequent Suzuki coupling with bromothiophene gives compound **5**. Compounds **2** and **5** were first lithiated and then treatment with sulfur and acetyl chloride which leads to formation of **3** and **6** in reasonable yields.

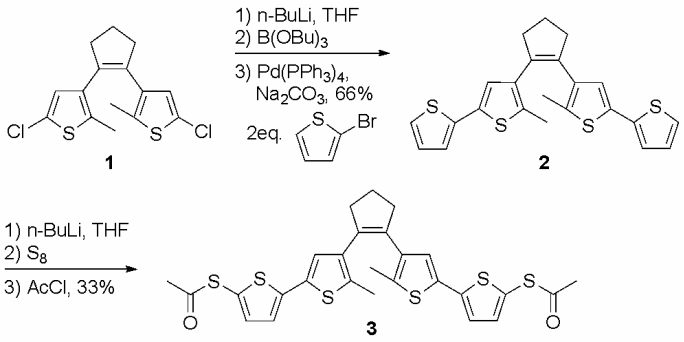

Scheme 1 *Synthetic route to compound* ***3.***

[†] J. H. Hurenkamp, thesis in preparation.

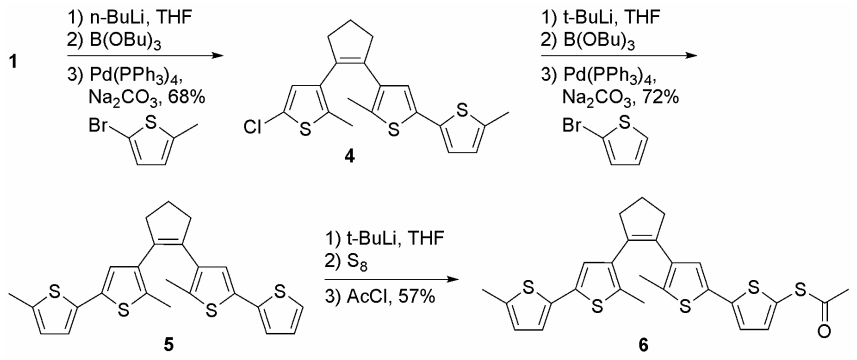

Scheme 2 *Synthetic route to compound* ***6****.*

Compounds **3** and **6**, like other dithienylethene-based molecular switches, can exist in two different forms, the so-called open and closed state (Figure 2). Upon irradiation with UV light the open form (dissolved in toluene) transform into the closed form with a high photoconversion (99%). When visible light is used the closed form returns quantitatively to the open form. In the open form, electronic interactions between two halves of the molecules are weak due to the lack of direct conjugation over both halves of the molecule. By contrast, the closed form allows π electrons to be delocalized over the whole linearly conjugated molecular backbone. As a consequence of the difference in π electron delocalization, the open form is colorless and the closed form is colored (Figure 2). The UV/Vis absorption spectra indicate that the HOMO-LUMO gaps of **3** and **6** are considerably reduced in their closed forms. Therefore, one can anticipate a major increase in conductance for the closed forms compared to the open forms.

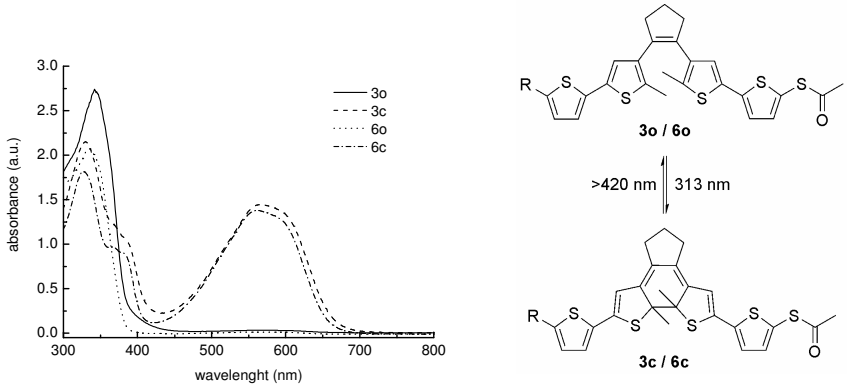

Figure 2 *UV/Vis absorption spectra of compounds* ***3*** *and* ***6*** *and photochemical interconversion of the open and closed forms. For* ***3*** *R is SAc and for* ***6*** *R is Me.*

2.3 Mechanically Controlled Break-Junction Experiment

In order to measure single molecule transport we use the mechanically controllable break-junction (MCBJ) technique.[9,11] A schematic illustration of the set-up for the technique is displayed in Figure 3. For MCBJ experiments, the molecular switches **3o** (open state) were first dissolved in tetrahydrofuran (THF). Upon irradiation with UV light (λ = 313 nm) switching to the closed form **3c** occurs. To prevent the molecules from switching back, all subsequent experiments were performed in the dark. A droplet of solution was introduced onto the break junction with a microsyringe. Once the molecules reach the gold, the protective acetyl groups split off and a self-assembled monolayer (SAM) is formed.[21] In principle, there are two approaches to achieve a molecular bridge. The first is to break the junction, open the electrodes far apart, and then form a SAM.[11] In this situation the system is in the tunneling regime and the resistance has an exponential dependence on the distance between the electrodes. Now we decrease the distance, applying a bias voltage of V = 1 V to assist a molecule to align between the electrodes, until we observe stable behavior. In the employed device, this always occurred at resistances of the order of MΩ, and it corresponds to the establishment of a Au-molecule-Au bridge.[11] The second approach is to first apply the solution and then open the wetted junction to form a molecular bridge.[9] Both methods were tested and the same results were observed.

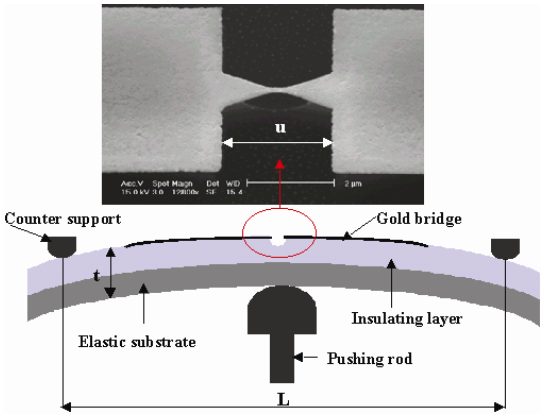

Figure 3 *The mechanically controllable break-junction (MCBJ) technique. Top: Scanning electron micrograph of the free standing gold bridge. Bottom: layout of the technique (not to scale). The whole device is 2 x 2 mm*^{2}.

Once the resistance is stabilized by molecular bridge formation, current-potential (IV) characteristics were measured (Figure 4a). The room temperature IV's (Figure 4a) do not show sharp features (see also Reichert et al.[11] and Heurich et al.[22]). After waiting for about half an hour, irradiation of the junction with λ = 546 nm light was begun, while monitoring the resistance as a function of time. In Figure 4b a typical result is shown. After a short time a sharp increase in the resistance is observed, attributed to switching of the molecule from the closed to the open form. The resistances we find after switching are in the GΩ range, about 3 orders of magnitude larger than the initial value. Such a ratio between the resistances of the open and closed form is in reasonable agreement with the work by Fraysse et al.,[23] who both calculated and measured the coupling through the switching unit in a similar molecule. In Figure 4c a typical IV curve obtained after switching is displayed. Also shown in Figure 4c is a fit to Stratton's tunneling formula (a schematic representation of electron tunneling in a polarized tunnel junction is shown in Chapter 6) $I = I_0 \sinh(eVd\sqrt{(m/2\hbar^2\varphi)})$ in which we put I_0 and φ as free parameters (m is the electron mass[24]). For d the calculated length of the open molecule (1.81 nm) was used. From the fit φ = 1.5 eV and $I_0 = 4 \times 10^{-11}$ A was found.

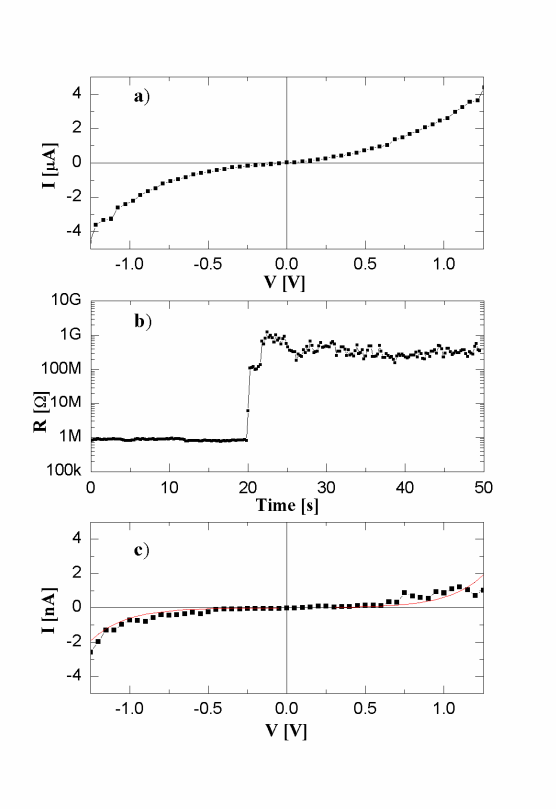

Figure 4 *MCBJ results. (a) Typical IV curve of the connected molecule in the closed form and (b) resistance versus time. At t = 0 a lamp is turned on (λ = 546 nm). After approximately 20 s a clear jump is observed (1 V bias). (c) Typical IV curve of the molecule after switching. The line is a fit to the Stratton formula (for details, see text).*

We observed the switching process ten times out of 12 attempts. The two times that were not successful a much lower concentration of the molecules in THF (0.15 mM) was used. In the other ten experiments we used a concentration of 1 to 2 mM. Switching times ranging from 10 s to 6 min, were observed.[25] After switching to the open state we attempted to switch the molecule back to the closed state by illuminating it with UV light (313 nm). However, this was unsuccessful. Since in solution the switching process from the open to closed state has a very high quantum yield (typically for similar compounds ~0.4 which is two orders of magnitude higher than from closed to open[26]) the absence of the reverse process seems to be related to the influence of the gold electrodes on the molecular system (see below).

One also has to consider other possibilities for a sharp jump in the resistance, such as migration of gold atoms or breaking of the gold thiol bonds. In order to exclude these possibilities additional experiments were performed: (a) illumination of the open junction without molecules and (b) illumination of molecular bridges formed by conjugated T3 molecules (three thiophene rings with two thiol end groups).[9] In these experiments such jumps in the resistance were not observed after the lamp was turned on (for at least 1 h).

2.4 STM Experiments

The break junction experiments on the dithiol thiophene-substituted diarylethene switch **3** described above yielded two main conclusions:

i) switching a molecule from the closed to the open state results in a significant resistance increase of over two orders of magnitude;

ii) once thiophene-based diarylethenes are connected to gold via the Au-S bond, they were found only be switching from the closed to the open form.

The nature of the break-junction experiment does not allow for direct determination of the number of molecules that are connecting two electrodes (if repetitive break-junction experiments are not performed with a subsequent statistical analysis). The conformation of the molecules and their binding position on break-junction electrodes, with unknown geometry, cannot be established precisely as well as the nature of environment that is surrounding them. It is known that "small" variations in the microscopic geometry of the contact may lead to significant variation in the measured conductance.[27] In order to understand charge transport through a molecule attached to electrodes the aforementioned issues have to be investigated. Many of these difficulties can be addressed when a molecule of interest is inserted into a self assembled alkanethiol monolayer with a relatively well-defined geometry.[28] A combination of STM and Scanning Tunneling Spectroscopy[13] present themselves techniques of choice to investigate the conductive properties of molecules and their surroundings.

To study individual thiophene-substituted switches **6**, a mixed self-assembled monolayer (SAM) of dodecanethiol (DT) and closed form switches **6c** was formed on atomically flat gold.[29] In Figure 5a, a constant current STM image of a mixed self-assembled monolayer is shown. In accordance with the literature,[30] a set of domains is observed, each consisting of an ordered alkanethiol lattice. The domains are separated by domain boundaries and by several lower areas. The latter 'islands' are one atomic gold step lower than their surroundings, but are also covered with alkanethiols. The key features, however, are the

small peaks (bright spots) that occur within the alkanethiol lattice. Since these spots are lacking when a sample has only been in a dodecanethiol solution, we associate them with the conjugated switches (single molecules or small aggregates of diarylethenes). An STM signal is a convolution of topography (real height) and local conductance.[30] Hence the apparent height difference (typically 0.25 nm) between **6c** and DT (molecular lengths 1.70 and 1.62 nm, respectively) is largely determined by the conductance properties of **6c** and DT. Since the conductance of the diarylethenes decreases considerably upon switching from closed to open forms, STM observes photochromic switching as a sudden decrease in the molecule's apparent height. This is associated with the disappearance of the bright spots upon irradiation (Figure 5c). To demonstrate such light induced switching, however, it is essential to separate light-induced switching from other switching effects. In recent years, several studies of statistical 'on–off' switching effects or 'blinking' during STM scanning have appeared, the origin of which is heavily debated.[30e-k]

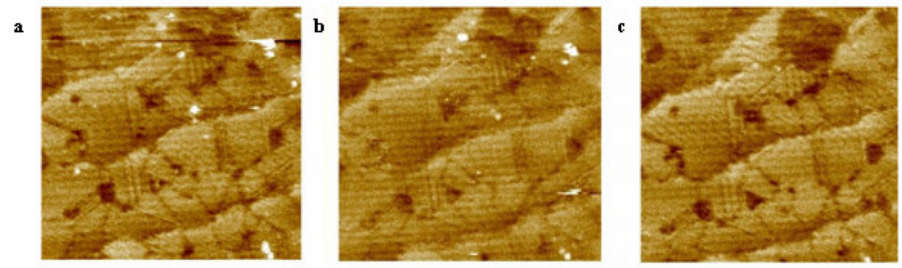

Figure 5 *Three STM images (77 x 74 nm^2, height scale: 1 nm; I_s=2 pA, V=0.75 V, taken in air, unfiltered zoomed images) of a DT SAM containing photochromic switches* ***6c****. Scanning in the dark begins at t=0, whereas at t=52 min illumination is started (300 W Xe lamp with high pass filter, δ>450 nm). Image a is taken at t=11.8 min. (dark), b at t=32 min. (dark) and c at t=77.7 min. (illuminated). Both stochastic switching (a to b) and photochromic switching (b to c) are observed. In c, after 25.7 min of illumination, almost all molecules have been converted to the open state.*

The following experiments (see Figure 5) were performed in order to study and separate stochastic and light-induced switching effects. First, a mixed DT-**6c** monolayer was scanned in the dark for typically 30 min (see Figures 5a and 5b). Detailed inspection of all images taken without illumination indeed revealed random "ON"-"OFF" switching. After scanning in the dark for a certain period (defined below), we turn on a 300 W Xe lamp with appropriate filtering. Scanning continued and increased switching to the "OFF" state was observed. This indicates photochromic switching from the conjugated to the non-

conjugated isomer. Finally, after 25.7 min of illumination, almost all photochromic switches have switched to the open form (see Figure 5(c)).

2.4.1 Stochastic switching

Since both stochastic and photochromic switching phenomena are present in our measurements, we choose to separate the data on the individual contributions using statistics. For each image taken, the number of molecules in the "ON" and "OFF" states was counted. Two different counting schemes were introduced to obtain additional information (see Figures 6a and 6b). In 'method A', all molecules that are "ON" within an STM image are counted (regardless of their position) and this number (N) was plotted versus time. Note that a molecule that was "OFF" at $t = 0$, but turns "ON" at a time t, is counted. In 'method B', we only focus on molecules that were 'on' at $t = 0$ and note their x, y-coordinates. For each later image we check if at these coordinates (within a few nm^2) there still is an "ON"-state molecule. If not (e.g., the molecule is "OFF", or has moved substantially) it is not counted. Note also that a molecule that is "OFF" initially, but 'on' at $t = \tau$, is not counted. We first focus on stochastic switching, i.e., exclusively on STM scanning in the dark. In Figure 6c, the normalized counting results for the sample in Figure 5 are displayed (diamonds, method A; squares, method B). For both methods, we recognize the 'blinking' effect in the statistical fluctuation of N on smaller timescales ('noise'). Furthermore, an initial decrease in N was observed until, after around 20 min, the number stabilizes. This decrease and stabilization is typical for experiments in the dark. There is quite a difference in final plateau values between methods A ($N/N_0 \rightarrow 0.78$) and B ($N/N_0 \rightarrow 0.26$). In fact, this is observed more generally. Figure 6d displays the normalized plateau values for all data sets as a function of STM bias voltage. At all biases, the plateau values for method A exceed those for method B, while both sets decrease with increasing bias voltages. To interpret this, both methods were associated with three possible effects: reversible stochastic switching (blinking), irreversible "ON"-to-"OFF" switching and diffusion.

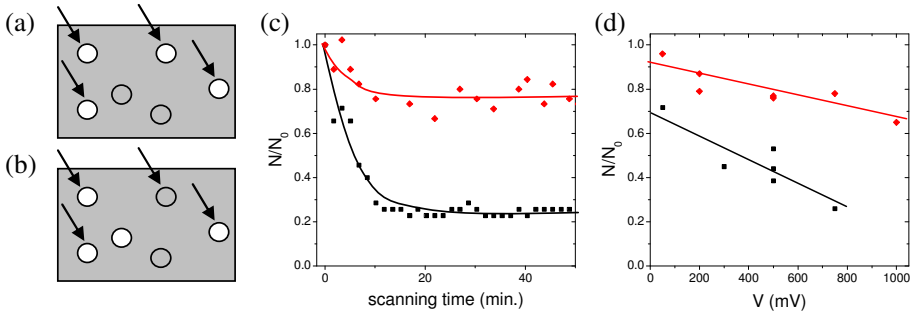

Figure 6 *Stochastic switching effects. Two methods of counting are used as illustrated in (a) and (b). In both (a) (at t=0) and (b) (at t=t) two molecules are "OFF" and four are "ON", but they are not the same ones. With method A, all "ON"-state molecules are counted regardless of history, giving N=4 for both (a) and (b), so that* $N_{(t)}/N_0=1$*. With method B, only the molecules that are 'on' at t=0 are followed, marked with an arrow, giving N=4 for (a) and N=3 for (b), so that* $N_{(t)}/N_0=3/4$*. (c) Normalized number of molecules in the "ON" state,* $N_{(t)}/N_0$*, vsersus time for the sample in Figure 5 (measured at 0.75 V). Diamonds: method A; squares: method B. After 20 min, a plateau in the number of counts is found, giving us two 'equilibrium values' for methods A (0.78) and B (0.26) (d) Equilibrium values versus bias for method A (diamonds) and method B (squares), determined for various samples. The "ON"-"OFF" ratio shifts to the "OFF"-state molecule side, if we scan at higher voltages. Lines are guides to the eye.*

First, let us suppose that reversible switching takes place only, and that its typical timescale is small (τ < 10 min). When the first image is recorded, we expect some of the conjugated molecules to be "ON" (N_{on}), and some to be "OFF" (N_{off}). Both in method A and B, we have $N_0 = N_{on}$ ($t = 0$). After a substantial period of scanning (>τ), some of the molecules that were first 'on' will have turned "OFF" and vice versa. However, N_{on} (which is the number counted in method A) and N_{off} are not expected to change. Hence, for method A, one expects $N_{(t)}/N_0 \approx 1$, i.e., no change except for statistical variations. (Interestingly, these fluctuations are found to increase with bias voltage themselves.) For method B, however, one follows a particular set of molecules (i.e. 'on' at $t = 0$). If some of these turn "OFF", the number counted decreases (regardless of others going from "OFF" to "ON"). At a time $t > \tau$, the spatial distribution of 'on' and 'off' states is randomized (though the numbers N_{on} and N_{off} have not changed). Hence $N_{(t)}/N_0$ approaches $N_{on}/(N_{on} + N_{off})$ for $t > \tau$, so that method B gives information about the dynamic equilibrium between "ON" and "OFF" states. Inspecting the images, we infer that this is the major contribution to the difference between

methods A and B (see below). Thus, Figure 6d implies that upon increasing the voltage bias ($V > 0$) the dynamic equilibrium between molecules in the "ON" and "OFF" states shifts to the "OFF" side. Although we have chosen a somewhat different method, our results can be compared to those of Lewis et al,[30h] who study conjugated molecules ('NPPB') in a functionalized alkanethiol SAM. They find the equilibrium to shift to the "OFF" state when the bias voltage is decreased from +1 to −1 V. However, since Lewis et al use functionalized conjugated molecules and alkanethiols, which interact via hydrogen bonding, the mechanism behind their results might be different.

Second, we look at the effect of irreversible "ON"-to-"OFF" switching. This would influence the results for both method A and B significantly: molecules that go to "OFF" and stay "OFF" are effectively taken out of the ensemble. Hence a decrease in the number of counts is now expected, especially for method A. This is indeed seen in Figure 6, though the effect is relatively small at low bias. Various origins for this irreversible switching can be thought of. One reason could be that due to the local environment the blinking time constant τ of some individual molecules exceeds the total scanning time, i.e., returning just takes too long.[30f-h] Furthermore, 'real' irreversible phenomena may occur. For diarylethenes, voltage and current-induced switching cannot be excluded. It has been shown that these molecules can switch due to a redox potential[31] or a current (provided excitons can be formed, which is unlikely in STM experiments).[32] In any case, N as counted by method A, appears to decrease rather smoothly with voltage. This is quite different from the work of Blum et al, who find a well defined switching voltage (from "OFF" to "ON") for 'BPDN' molecules.[30k]

Third, we consider the influence of diffusion. If a molecule moves away from its original spot by more than a few nanometres, it is no longer counted in method B (but still in method A). We note that spontaneous random walking will be quite limited. It is likely for a **6c** molecule to hop only if there is a vacancy or defect in the dense DT lattice. Indeed, at biases up to 0.5 V, we do not observe significant random walk. For experiments at higher bias, however, it appears that some molecules do shift position leading to a lower plateau value within method B. Possibly the large fields around the tip are able to help the **6** molecules overcome the diffusion barrier.

There is still no consensus on the origin of stochastic switching.[30f-k] The Weiss group has provided evidence for conformational switching in particular molecules, e.g. by looking at the influence of the alkanethiol matrix density on blinking.[30f-h] Nevertheless, stochastic switching appears in almost any system consisting of individual molecules inserted in an alkanethiol SAM. Hence, there must also be an additional, more general origin. Since STM measures a convolution of conductance and real height, either could be important here.

Ramachandran *et al*. relate the phenomenon to instabilities of the Au–S bond.[30i] A drawback of the latter explanation is that the energy scales do not seem to match. As noticed, the Au–S bond has a strength of 1.6 eV, whereas the typical energy scale for stochastic switching is found to be ~0.1 eV. As a possible way out, one could consider temporary disulfide formation (between the alkanethiol and the inserted molecule). This would loosen the Au–S bond with an energy barrier much lower than 1.6 eV. It should be noted, however, that the data of Donhauser *et al.* do not support such a model: instead of increased switching to a denser SAM (as expected for the disulfide picture), they see the opposite.[30f,g] In our opinion, the most general and hence most probable explanation for stochastic switching is that it is due to orientational changes, in particular changes in the tilt angle of the molecule.[30j] These can either be spontaneous or the result of the strong electric field between tip and substrate (~GV m^{-1}). The fact that we see a shift in the dynamic equilibrium (as well as increased fluctuations for increasing voltages) hints in this direction. Unfortunately, it appears difficult to find conclusive evidence for any of the mechanisms above. It is important to note, however, that stochastic switching has an origin different from photochromic switching. In the latter case, light-induced ring opening results in loss of the conjugation within the molecule, leading to a significant increase of resistance.

2.4.2 Photochromic switching

Having characterized stochastic switching in our samples, we turn to light-induced conductance switching. After scanning in the dark until a stable number *N* (method A) is reached, illumination was started to switch the closed switchable molecules to the open form. In Figure 7, the number of "ON"- state molecules **6** as a function of time for two series of STM experiments is displayed. It is observed that the number of "ON" molecules starts decreasing as soon as illumination starts. We relate this to photochromic switching from the closed to the open state, leading to a lower conductance and, consequently, a lower apparent height. The decrease in *N* is smooth and goes, roughly, exponentially with time. This is indeed what one expects for photochromic switching since each event is independent. We find decay half times of typically 30 min for the switches in the mixed SAM. This number is rather large compared to the conversion time measured for free closed switches in THF. For the same lamp and filtering, the half time in solution is a few minutes.[33] However, the half times for switching in a mixed SAM do compare well with those obtained for solutions of gold colloids covered by a monolayer of closed switches. For the latter we find a decay half time of around 40 min.[33] Coupling to gold appears to reduce the switching efficiency (from the closed to the open state), but, importantly, it does not completely hamper the conversion.

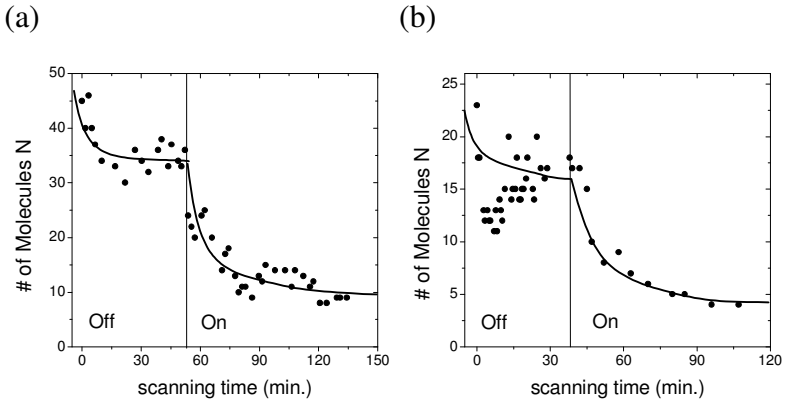

Figure 7 *Number of molecules in the 'on' state versus time (min), determined from two series of STM-images taken in air, both in the dark and during illumination (300 W Xe lamp). Counting is done using Method A. In (a) (same sample as in Figure 5), the lamp is turned on after 52 min (high pass filter, δ > 450 nm). (I_s = 2 pA, V = 0.75 V). In (b), the lamp (band pass filter around 550 nm) is turned on after 38 min (I_s = 30 pA, V = 1.0 V). Lines are guides to the eye.*

Since illumination of our sample may lead to spurious effects, the experiment will be discussed in more detail. First, heating may take place, leading to expansion effects. Although this could instantaneously change the tip–surface distance, the feedback loop will immediately correct for this. Furthermore, a temperature increase could lead to faster stochastic switching (lower τ).[30i] However, this would not lead to different counting statistics and, hence, it cannot explain the decrease observed in Figure 7. Second, light-induced Au–S bond breaking might occur, removing both alkanethiols and switches from the surface. For visible light, however, this is not expected and we do not see any evidence for it in our STM scans. After photochromic switching the molecules are still present.

We find that molecules in the open form (**6o**) have an apparent height that is approximately 0.2 nm lower than that of the closed form. Since the open conformer is in average slightly longer (by 0.1 nm) than its closed counter part, we have an apparent height change of 0.3 nm. It is instructive to compare this number to the conductance change measured in the break junction experiments.[33] For constant current STM, we can do this by setting $G_c \exp(-2\kappa d_c) = G_o \exp(-2\kappa d_o)$.[30c,34] Here G_c (G_o) denotes the conductance of the closed (open) form, d is the distance between tip and molecule, and κ is the tunnel decay constant between tip and molecule. Taking $G_c/G_o \sim 200$, we obtain the right apparent height

difference, i.e. $d_c - d_o = 0.3$ nm, if we use $\kappa = 8.8$ nm^{-1}. The latter number corresponds to a tunnel barrier height of 3 eV, which is reasonable. We note however that it is difficult to quantify the exact conductance change associated with switching, since we have no independent information regarding the molecular tilt angles.

Unfortunately, the thiophene-based diarylethenes used in this study as well as in reference 33 have an important drawback. Whereas switching is reversible in solution, the situation changes once these molecules are connected to gold via a thiol bond. In the latter case, switching from the closed to the open form is still possible, but from open to closed is not.

2.5 The Origin of Irreversibility

To rationalize these findings regarding irreversibility of the switching process for the switches covalently attached to gold electrodes, the switching process of compound **3** was investigated theoretically and the influence of gold on the switching discussed qualitatively. For this, potential curves were calculated using a selection of semiempirical quantum chemical computational methods implemented in the HYPERCHEM 6.0 program package. The ground state and excited state potential curves were generated in a procedure in which the switching coordinate q (the distance between the carbon atoms which are responsible for the ring closure process) was changed in a systematic way between 0.13 and 0.4 nm (calculated distances for the closed and open form are 0.15 and 3.5 nm). In Figure 8 we plot, as a function of q, the ground state and excited state energy of the molecule **3** with respect to the vacuum level. The ground state and excited state profiles shown here are very similar to the results obtained by Ern et al.[35] using a different method. In Figure 8 the paths for ring opening and closure are drawn for the isolated molecule upon optical excitation in the UV and visible spectral region. Clearly the ring opening process is expected to have a lower quantum yield than the reverse process, due to the presence of a barrier.[26] To consider the influence of gold on the molecular system, we have also plotted the Fermi level of polycrystalline gold (5.3 eV with respect to the vacuum level) in Figure 8.[36] We relate the failure of the closing process to the proximity of the gold Fermi level and the excited state molecular energy for $0.22<q<0.25$ nm. As a consequence, an efficient mixing of the gold states and the first excited molecular electronic state is expected, taking place at the right side of the ground state maximum. This results in quenching of the excited open state inhibiting the ring closure process. The electronic excited state involved in the ring opening process, on the other hand, is separated by more than 1 eV from the gold Fermi level. Hence, the ring opening process is not inhibited.

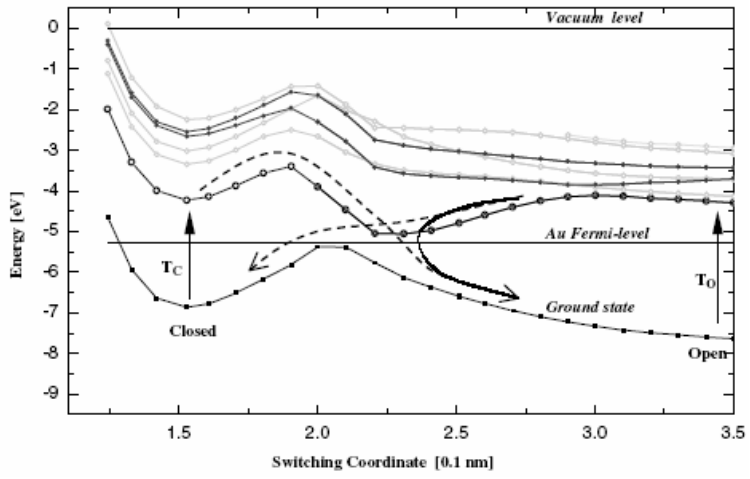

Figure 8 *Potential energy curves of the molecular switch* ***3*** *along the switching coordinate q (black lines: optically allowed states; gray lines: optically forbidden excited states). The vacuum level is set at 0 eV. The switching process is initiated by an excitation to the first excited state (T_c; T_o). For a molecule in solution, the evolution of the switching process is indicated with dashed arrows. For a molecule connected to gold, however, the potential curve of the first excited state comes very close to the Au Fermi level (at 0.22<q<0.25 nm), resulting in an efficient mixing of these respective states. When the open molecule goes to the first excited state (T_o), the closing process sets in, i.e., the excited state potential curve is followed towards lower q (solid arrow). However, when 0.22<q<0.25 nm, the interaction with the gold makes the excited molecule relax back to the ground state (at the right side of the local maximum), and hence back to the open form. As a consequence there is no switching from the open to the closed form.*

An intention of the presented *ad hoc* calculations[37] was to explain the behavior observed by focusing on potential energy curves of the switching and the role of the gold Fermi level. Major drawbacks of these calculations are that the semiempirical approach has been used and an effect of a gold anchoring on molecular energy levels has been neglected. Based on our break-junction experiment results also other groups tried to explain the lack of reversibility for the molecule **3** connected to gold. Li *et al*.[38] calculated HOMO and LUMO levels of model diarylethene molecules connected to small gold clusters using a density functional theory (DFT) based method. Comparing alignments of the metal Fermi level and the HOMO and LUMO orbitals of the open and closed isomers they found that the HOMO of the open isomer is buried more than 1 eV beneath the metal Fermi level near to the fast increasing edge of the 3D bands of Au (where the Au density of states is high). In contrast,

the HOMO of the closed isomer is within the low density of states *s* band near the Au Fermi level. Li *et al*. speculate that the observed quenching of the ring closure reaction may result from the Fermi-level alignment in the open isomer. The deep lying HOMO level at a high metal density of states offers the opportunity for many possible electron transfer events, thus reducing the lifetime of the hole created after an excitation. Using DFT calculations Zhuang *et al*.[39] came to the similar conclusions investigating how strongly the HOMO orbitals of the open and closed isomers are mixed with orbitals of a contact electrode. They show that orbitals of the open form are strongly mixed with contact orbitals. As a consequence, it is not possible to empty the molecular HOMO by photoexcitation; it will simply be refilled with contact electrons. The HOMO stabilizes the open isomer compared to the closed one. On the other hand, the HOMO of the isolated closed isomer keeps its identity when attached to the gold contacts and a mixing of orbitals is low. These two theoretical approaches[38,39] offered an alternative explanation for the observed experimental results.

2.6 Conclusions

Based on the presented results it has been demonstrated that diarylethenes are promising candidates for molecular electronics. An ease of synthetic accessibility and addressability makes this an ideal system for many studies. UV/Vis measurements performed in toluene show that the open and closed forms can be addressed selectively resulting in the interconversion between both forms. Using MCBJ and STM diarylethene molecules have been incorporated between metallic nanoelectrodes and thus single molecule switching devices have been realized although so far only in one direction. Both methods confirm the dramatic decrease in conductance of the molecules when the closed form transforms to the open form upon an irradiation with visible light. Both sets of measurements show that for the molecules covalently connected to gold the switching occurs only in one direction, from the closed to the open form. The latter is attributed to quenching of the first excited state of the open form under the influence of gold. In the following chapters (4 and 5) an effect of spacer unit, connecting the central switching unit with anchoring groups, on the switching reversibility will be discussed.

2.7 Experimental Section

General Remarks

Reagents and starting materials were used as obtained from Aldrich and Acros Chimica, Fluka or Merck. ^{1}H NMR spectra were recorded on a Varian VXR-300 spectrometer (at 300 MHz) at ambient temperature. ^{13}C NMR spectra were recorded on a Varian VXR-300 (at 75.4 MHz). Chemical shifts are denoted in δ (ppm) referenced to the residual $CHCl_3$ peaks. Coupling constants *J*, are denoted in Hz. The splitting patterns are designated as following: s (singlet), d (doublet), t (triplet), q (quartet), m (multiplet) and b (broad). Mass spectra were recorded with a Joel JMS-600 mass spectrometer by Mr. A. Kiewiet with ionisation according to CI^+, DEI, EI^+ procedures. UV measurements were performed on a Hewlett-Packard HP 8453 FT spectrophotometer using UVASOL grade solvents (Merck). Aldrich, silica gel, Merck grade 9385, (230-400 mesh) was used for column chromatography. If necessary, solvents were distilled and dried before use by standard methods. Irradiations were performed with a 180 W Oriel Hg-lamp adapted with a suitable Mercury line filter for 313 nm and 546 nm irradiations (typical bandwidth 10 nm) and a cut-off (420 nm) filter for visible irradiation. Photostationary states are ensured by monitoring composition changes in time by taking UV spectra at distinct intervals until no further changes were observed.

Mechanically Controlled Break-Junction Experiments

The break-junction experiments were performed by Dr. D. Dulić and Dr. S. J. van der Molen. The device was patterned on an elastic phosphor bronze substrate covered with a thin insulating layer of polyimide by electron beam lithography. The device is made of gold and has a narrow neck in the middle (see Figure 3). After the gold deposition the polyimide below the bridge is removed, leaving behind a freestanding gold bridge. The bridge was broken by bending with a three-point bending mechanism. We obtain a mechanical ''attenuation factor'' [40] $r = 6tu/L^2 = 1{:}7 \times 10^{-5}$, for our device, where $t = 0.42$ mm is the substrate thickness, $u = 2.4$ μm the suspended length of the bridge, and $L = 18.8$ mm the distance between the counter supports. This provides control of the spacing between the electrodes with a precision of 10 pm. The two open ends form point contacts to which the molecules will be attached via the thiol groups that form a strong chemical bond with gold. Prior to the experiments with the molecules a number of devices were calibrated in ambient and argon atmosphere. We obtained an exponential increase of the resistance upon increase of the distance between the electrodes which is characteristic of the tunneling regime for the metal-air-metal junction. The $R(d)$ data were used, where the distance d was taken from the geometrical formula, to obtain an average value of the work function of gold $\langle\varphi\rangle = 6 \pm 2$ eV. This is in reasonable agreement with the experimental work function for gold which is 5.3 eV. Furthermore, IV characteristics were measured which can be satisfactorily fitted to the Simmons[41] and Stratton[42] formulas.

STM Experiments

The STM experiments were performed by Dr. S. J. van der Molen. For monolayer formation, *n*-dodecanethiol was purchased from Aldrich. Flat gold layers are created using the procedure described in reference 29. Within atomically flat plateaus, the herringbone structure was observed.[43] Two SAM preparation methods are chosen. For the first ('exchange reaction method'), a gold sample was put in a solution of dodecanethiol in ethanol (concentrations ranging from 1 to 100 mM) for 4 to 24 h (at 295 K). Next, the solution was heated to 351K for 2 h. Finally, the sample was put in ethanol containing closed switches (concentration 1 mM) for 4 h. For the second method, we directly prepare the SAM from a mixture of DT (95–99 molecular %) and **6** in ethanol ('co-adsorption method'). STM measurements were performed in air with a Digital Instruments Multimode scanner with a Nanoscope IV controller, purchased from Veeco. Illumination of the SAMs was performed with a 300 W Xe lamp (purchased from LOT-Oriel), with appropriate filtering and fiber optics.

Details on Semiempirical Calculations

The potential curves were calculated by Dr. H. T. Jonkman using a selection of semiempirical quantum chemical computational methods implemented in the HYPERCHEM 6.0 program package (provided by Hypercube, Inc). The total energy was calculated with the AM1 quantum chemical semiempirical method. For each q, the geometry of the molecule was fully optimized using a conjugate gradient procedure (Polak-Ribiere). The singlet excited state manifold was calculated with the Zerner intermediate neglect of differential overlap/spectroscopy method in which ten occupied and ten unoccupied orbitals were incorporated in the single excited state configuration interaction procedure. The vacuum level is here defined as the total energy of the molecule with one electron removed; i.e., it is equal to the ionization potential of the molecule. Within Koopman's theorem, this ionization potential is representative for the position of the highest occupied molecular orbital (HOMO) of the molecule. In the same approximation the energy of the electron addition state (electron affinity) is the energy of the lowest unoccupied molecular orbital (LUMO). In that description the optical and conduction gap coincide and the first excited state mimics the HOMO-LUMO gap.

1,2-Bis[2-methyl-5-(thien-2-yl)thien-3-yl]cyclopentene (2)

To a solution of compound **1**[20] (240 mg, 0.729 mmol) in THF (7 mL), kept under an inert N_2 atmosphere, *n*-BuLi (1.2 mL of 1.6 M solution in *n*-hexane, 1.92 mmol) was added. After 1h, $B(OBu)_3$ (0.05 mL, 2.19 mmol) was added and the mixture was stirred for 1h to produce a boronic ester intermediate. In a separate flask 2-bromo-5-methylthiophene (0.287

mL, 2.96 mmol), $Pd(PPh_3)_4$ (0.096 mg, 0.083 mmol), THF (5 mL), 2M Na_2CO_3(aq.) (4 mL) and ethylene glycol (5 drops) were preheated to 80 °C and the boronic ester solution was added slowly. The reaction mixture was heated under reflux overnight, diluted with diethyl ether (50 mL) and washed with water (50 mL). The aqueous layer was washed with an additional volume of ether (50 mL) and the combined organic phases were dried over Na_2SO_4 and concentrated. Subsequent chromatography on silica gel (*n*-hexane) afforded compound **2** (203 mg, 66 %). mp. 204-208°C (dec.) ^{1}H NMR (300MHz, $CDCl_3$) δ 1.94 (s, 6H), 2.04 (m, 2H), 2.79 (t, *J* = 12.5 Hz, 4H), 6.87 (s, 2H), 6.95 (t, *J* = 6.5 Hz, 2H), 7.03 (d, *J* = 4.5 Hz, 2H), 7.13 (d, *J* = 8.5 Hz, 2H) ppm. ^{13}C NMR (75.4 MHz, $CDCl_3$): δ 14.3 (q), 22.9 (t), 38.5 (t), 122.9 (d), 123.7 (d), 124.5 (d), 127.6 (d), 133.0 (s), 134.0 (s), 134.5 (s), 136.3 (s) ppm. HRMS calcd. for $C_{23}H_20S_4$ 424.045, found 424.045.

1,2-Bis[5-(5-acetylsulfanylthien-2-yl)-2-methylthien-3-yl]cyclopentene (3)

Compound **2** (100 mg, 0.236 mmol) was dissolved in THF (5 ml) and the solution was cooled to -80 °C. To this solution was added dropwise *n*-BuLi (0.4 ml of 1.6 M solution in hexane, 0.64 mmol). After 2h S_8 (15 mg, 0.469 mmol) dissolved in THF (1 ml) was added and the mixture was allowed to reach slowly room temperature. After 2h the reaction mixture was cooled to 0 °C and acetyl chloride (0.068 ml, 0.952 mmol) was added. After 3h the mixture was diluted with dichloromethane, washed with water and the organic phase dried (Na_2SO_4) and concentrated. Subsequent chromatography (*n*-hexane / dichloromethane 7:2) afforded compound **3** (41 mg, 33 %). mp. 204-208°C (dec.) ^{1}H NMR (500MHz, $CDCl_3$) δ 1.93 (s, 6H), 2.04 (m, 2H), 2.40 (s, 6H), 2.78 (t, *J* = 7.5 Hz, 4H), 6.88 (s, 2H), 7.00 (d, 2H), 7.34 (d, 2H) ppm. ^{13}C NMR (75.4 MHz, $CDCl_3$): δ 14.5 (q), 23.0 (t), 29.6 (q), 38.6 (t), 122.7 (d), 123.2 (s), 123.3 (s), 125.1 (s), 125.2 (s), 132.2 (d), 134.4 (d), 136.4 (s), 136.5 (s), 136.6 (s) ppm. MS (EI): 572 [M+]; HRMS calcd. for $C_{27}H_{24}O_2S_6$ 572.010, found 572.010.

1-(5-Chloro-2-methylthien-3-yl)-2-[5-(5-methylthien-2-yl)-2-methylthien-3-yl]cyclopentene (4)

To a solution of compound **1** (2.25 g, 6.83 mmol) in THF (100 mL), kept under an inert N_2 atmosphere, *t*-BuLi (4,70 mL of 1.6 M solution in *n*-hexane, 7.51 mmol) was added. After 1h, $B(OBu)_3$ (2.77 mL, 10.3 mmol) was added and the mixture was stirred for 1h to produce a boronic ester intermediate. In a separate flask 2-bromo-5-methylthiophene (1.56 mL, 13.66 mmol), $Pd(PPh_3)_4$ (0.237 g, 0.21 mmol), THF (23 mL), 2M Na_2CO_3(aq.) (18 mL) and ethylene glycol (20 drops) were preheated to 80 °C and the boronic ester solution was added slowly. The reaction mixture was heated under reflux overnight, diluted with diethyl ether (200 mL) and washed with water (200 mL). The aqueous layer was washed with an additional volume of ether (200 mL) and the combined organic phases were dried

over Na_2SO_4 and concentrated. Subsequent chromatography on silica gel (*n*-hexane) afforded compound **4** as a sticky oil (1.82 g, 68 %). ^{1}H NMR (300 MHz, $CDCl_3$): δH 1.88 (s, 3H), 1.93 (s, 3H), 1.98-2.08 (m, 2H), 2.46 (s, 3H), 2.71-2.80 (m, 4H), 6.61-6.62 (m, 2H), 6.76 (s, 1H), 6.48 (d, *J*=3.7 Hz, 1H) ppm. ^{13}C NMR (75.4 MHz, $CDCl_3$): δC 14.1 (q), 14.2 (q), 15.3 (q), 22.8 (t), 38.3 (t), 38.4 (t), 122.8 (d), 123.6 (d), 125.0 (s), 125.7 (d), 126.8 (d), 133.2 (s), 133.4 (s), 133.5 (s), 133.8 (s), 135.0 (s), 135.3 (s), 135.9 (s), 138.5 (s), ppm. HRMS: calcd. for $C_{21}H_{19}S_2Cl$ 370.062, found 370.063.

1-[2-Methyl-5-(5-methylthien-2-yl)thien-3-yl]-2-[2-methyl-5-(thien-2-yl)thien-3-yl]cyclopentene (5)

To a solution of compound **4** (1.34 g, 3.43 mmol) in THF (50 ml), kept under an inert N_2 atmosphere, *t*-BuLi (2.74 ml of 1.5 M solution in *n*-pentane, 4.11 mmol) was added. After 1h, $B(OBu)_3$ (1.39 ml, 5.15 mmol) was added and the mixture was stirred for 1h to produce a boronic ester intermediate. In a separate flask 2-bromothiophene (0.66 ml, 6.86 mmol), $Pd(PPh_3)_4$ (0.119 g, 0.10 mmol), THF (19 ml), (aq.) 2M Na_2CO_3 (13 ml) and ethylene glycol (18 drops) were preheated to 80 ^{o}C and the boronic ester solution was added slowly. The reaction mixture was heated under reflux overnight, diluted with diethyl ether (200 ml) and washed with water (200 ml). The aqueous layer was washed with an additional volume of ether (200 ml) and the combined organic phases were dried over Na_2SO_4 and concentrated. Subsequent chromatography on silica gel (*n*-hexane) afforded compound **5** as a sticky oil (1.08 g, 72 %). ^{1}H NMR (300 MHz, $CDCl_3$): δ = 1.96 (s, 3H),1.97 (s, 3H), 2.05-2.10 (m, 2H), 2.47 (s, 3H), 2.82 (t, *J*=7.7 Hz, 4H), 6.63 (d, *J*=3.7 Hz, 1H), 6.82 (s, 1H), 6.85 (d, *J*=3.7 Hz, 1H), 6.91 (s, 1H), 6.98-7.00 (m, Hz, 1H), 7.07 (d, *J*=3.3 Hz, 1H), 7.16 (d, *J*=5.1 Hz, 1H) ppm. ^{13}C NMR (75.4, $CDCl_3$): δ = 13.8 (q), 14.9 (q), 22.5 (t), 38.0 (t), 122.3 (d), 122.4 (d), 123.1 (d), 123.2 (d), 124.0 (d), 125.3 (d), 127.1 (d), 132.5 (s), 134.9 (s), 133.0 (s), 133.5 (s), 133.9 (s), 134.1 (s), 134.9 (s), 135.7 (s), 135.9 (s), 137.3 (s), 138.0 (s) ppm. HRMS: calcd. for $C_{24}H_{22}S_4$ 438.060, found 438.062.

1-[5-(5-Acetylsulfanylthien-2-yl)-2-methylthien-3-yl]-2-[2-methyl-5-(5-methylthien-2-yl)thien-3-yl]cyclopentene (6)

Compound **5** (1 g, 2.28 mmol) was dissolved in THF (50 ml) and the solution was cooled to -80 ^{o}C. To this solution was added dropwise *t*-BuLi (1.82 ml of 1.5 M solution in *n*-pentane, 2.74 mmol). After 2h S_8 (0.073 g, 2.28 mmol) dissolved in THF (4 ml) was added and the mixture was allowed to reach slowly room temperature. After 2h the reaction mixture was cooled to 0 ^{o}C and acetyl chloride (0.32 ml, 4.56 mmol) was added. After 3h the mixture was diluted with dichloromethane, washed with water and the organic phase dried (Na_2SO_4) and concentrated. Subsequent chromatography (*n*-hexane / dichloromethane 7:2) afforded compound **6** (0.67 g, 57 %) as a sticky oil. ^{1}H NMR (300 MHz, $CDCl_3$): δ =

1.95 (s, 3H), 1.97 (s, 3H), 2.07-2.10 (m, 2H), 2.42 (s, 3H), 2.47 (s, 3H), 2.81 (t, *J*=7.3 Hz, 4H), 6.63 (d, *J*=3.3 Hz, 1H), 6.81 (s, 1H), 6.85 (d, *J*=3.3 Hz, 5H), 6.93 (s, 1H), 7.03 (s, 2H) ppm. ^{13}C NMR (75.4, $CDCl_3$): δ = 14.2 (q), 14.3 (q), 15.3 (q), 22.9 (t), 29.4 (q), 38.4 (t), 122.7 (s), 122.8 (d), 123.2 (d), 123.7 (d), 125.3 (d), 125.7 (d), 132.1 (s), 133.3 (s), 133.5 (s), 134.1 (s), 134.9 (s), 135.0 (s), 135.3 (s), 136.0 (s), 136.5 (s), 136.6 (d), 138.4 (s), 144.1 (s), 194.3 (s) ppm. HRMS: calcd. for $C_{26}H_{24}OS_5$ 512.125, found 512.124.

2.8 References and Notes

[1] a) C. Joachim, J. K. Gmizewski and A. Aviram, *Nature* **2000**, *408*, 541-548; b) R. L. Carroll and C. B. Gorman, *Angew. Chem. Int. Ed*. **2002**, *41*, 4378-4400.

[2] S. Fraysse, Ch. Coudret and J.-P. Launay, *Eur. J. Inorg. Chem*. **2000**, 1581-1590; B. Jousselme, P. Blanchard, N. Gallego-Planas, E. Levillain, J. Delaunay, M. Allain, P. Richomme and J. Roncali, *Chem. Eur. J*. **2003**, *9*, 5297-5306.

[3] M.-K. Ng and L. Yu, *Angew. Chem. Int. Ed.* **2002**, *41*, 3598-3601.

[4] N. Robertson and C. A. McGowan, *Chem. Soc. Rev*. **2003**, *32*, 96-103.

[5] H. Yu, Y. Luo, K. Beverly, J. F. Stoddart, H.-R. Tseng and J. R. Heath, *Angew. Chem. Int. Ed.* **2003**, *42*, 5706-5711; A. Babel, S. A. Jenekhe, *J. Am. Chem. Soc*. **2003**, *125*, 13656-13657.

[6] J. E. Green, J. W. Choi, A. Boukai, Y. Bunimovich, E. Johnston-Halperin, E. DeIonno, Y. Luo, B. A. Sheriff, K. Xu, Y. S. Shin, H. –R. Tseng, J. F. Stoddart, J. R. Heath, *Nature* **2007**, *445*, 414-417.

[7] B. L. Feringa, *Molecular switches*, Wiley, Weinheim, Germany, **2001**.

[8] a) M. Irie, in *Molecular switches*, B. L. Feringa, Wiley, Weinheim, Germany, **2001**, pp. 37-62; b) M. Irie, *Chem. Rev*. **2000**, *100*, 1685; c) H. Tian and S. Yang, *Chem. Soc. Rev.* **2004**, *33*, 85.

[9] C. Kergueris, J.-P. Bourgoin, S. Palacin, D. Esteve, C. Urbina, M. Magoga and C. Joachim, *Phys. Rev. B* **1999**, *59*, 12505-12513; M. Mayor, H. B. Weber, J. Reichert, M. Elbing, C. von Hänisch, D. Beckmann, M. Fisher, *Angew. Chem. Int. Ed.* **2003**, *42*, 5834-5838.

[10] K. W. Kittredge, M. A. Fox and J. K. Whitesell, *J. Phys. Chem. B* **2001**, *105*, 10594; A. Ishida, Y. Sakata and T. Majima, *Chem. Commun.* **1998**, 57.

[11] J. Reichert, R. Ochs, D. Beckmann, H. B. Weber, M. Mayor, H. von Lohneysen, *Phys. Rev. Lett.* **2002**, *88*, 176804.

[12] H. Park, J. Park, A. K. L. Lim, E. H. Anderson, A. P. Alivisatos, P. L. McEuen, *Nature* **2000**, *407*, 57-60.

[13] a) P. Jiang, G. M. Morales, W. You, L. Yu, *Angew. Chem. Int. Ed*. **2004**, *43*, 4471-4475; b) J. He, Q. Fu, S. M. Lindsay, J. W. Ciszek, J. M. Tour, *J. Am. Chem. Soc*. **2006**, *128*, 14828-14835; c) L. A. Bumm, J. J. Arnold, T. D. Dunbar, D. L. Allara, P. S. Weiss, *J. Phys. Chem. B* **1999**, *103*, 8122-8127; d) B. Xu, N. J. Tao, *Science* **2003**, *301*, 1221-1223.

[14] D. J. Wold, C. D. Frisbie, *J. Am. Chem. Soc*. **2001**, *123*, 5549-5556; D. J. Wold, R. Haag, M. A. Rampi, C. D. Frisbie, *J. Phys. Chem. B* **2002**, *106*, 2813-2816; X. D. Cui, X. Zarate, J. Tomfohr, O. F. Sankey, A. Primak, A. L. Moore, T. A. Moore, D. Gust, G. Harris, S. M. Lindsay, *Nanotechnology* **2002**, *13*, 5-14; X. D. Cui, A. Primak, X. Zarate, J. Tomfohr,O. F. Sankey, A. L. Moore, T. A. Moore, D. Gust, L. A. Nagahara, S. M. Lindsay, *J. Phys. Chem. B* **2002**, *106*, 8609-8614.

[15] M. Mahadevan, R. M. Bradley, *Phys. Rev. B* **1999**, *59*, 11037-11046.

[16] J. G. Kushmerick, D. B. Holt, S. K. Pollack, M. A. Ratner, J. C. Yang, T. L. Schull, J. Naciri, M. H. Moore, R. Shashidhar, *J. Am. Chem. Soc*. **2002**, *124*, 10654-10655.

[17] R. Holmlin, R. Haag, M. L. Chabinyc, R. F. Ismagilov, A. E. Cohen, A. Terfort, M. A. Rampi, G. M. Whitesides, *J. Am. Chem. Soc*. **2001**, *123*, 5075-5085; M. A. Rampi, G. M. Whitesides, *Chem. Phys*. **2002**, *281*, 373-391; K. Slowinski, H. K. Y. Fong, M. Majda, *J. Am. Chem. Soc.* **1999**, *121*, 7257-7261; R. L. York, P. T. Nguyen, K. Slowinski, *J. Am. Chem. Soc.* **2003**, *125*, 5948-5953.

[18] H. B. Akkerman, P. W. M. Blom, D. M. de Leeuw, B. de Boer, *Nature* **2006**, *441*, 69-72.

[19] C. Zhou, M. R. Deshpande, M. A. Reed, L. Jones II, J. M. Tour, *Appl. Phys. Lett*. **1997**, *71*, 611-613; J. Chen, M. A. Reed, A. M. Rawlett, J. M. Tour, *Science* **1999**, *286*, 1550-1552; K. S. Ralls, R. A. Buhrman, R. C. Tiberio, *Appl. Phys. Lett*. **1989**, *55*, 2459-2461.

[20] L. N. Lucas, J. van Esch, R. M. Kellogg, B. L. Feringa, *Chem. Commun*. **1998**, 2313–2314; L. N. Lucas, J. J. D. de Jong, J. H. van Esch, R. M. Kellogg, B. L. Feringa, *Eur. J. Org. Chem.* **2003**, 155-166.

[21] J. M. Tour, L. Jones II, D. L. Pearson, J. J. S. Lamba, T. P. Burgin, G. M. Whitesides, D. L. Allara, A. N. Parikh, S. V. Atre, *J. Am. Chem. Soc*. **1995**, *117*, 9529-9534.

[22] J. Heurich, J. C. Cuevas, W. Wenzel, G. Schon, *Phys. Rev. Lett*. **2002**, *88*, 256803.

[23] S. Fraysse, C. Coudret, J. P. Launay, *Eur. J. Inorg. Chem*. **2000**, *7*, 1581-1590.

[24] Here we assume the effective mass m = 9.1 x 10^{-31} kg, in contrast to W.Wang, T. Lee, M. A. Reed., *Phys. Rev. B* **2003**, *68*, 035416.

[25] The switching times were somewhat dependent on the lamp employed; a 300 W Xe lamp gives lower times than a 200 W Hg lamp.

[26] P. R. Hania, R. Telesca, L. N. Lucas, A. Pugzlys, J. van Esch, B. L. Feringa, J. G. Snijders, K. Duppen, *J. Phys. Chem. A* **2002**, *106*, 8498-8507.

[27] S. M. Lindsay, *Faraday Discuss*. **2006**, *131*, 403-409; K. Stokbro, J. L. Mozos, P. Ordejon, M. Brandbyge, J. Taylor, *Comput. Mater. Sci*. **2003**, *27*, 151-156.

[28] X. D. Cui, A. Primak, X. Zarate, J. Tomfohr, O. F. Sankey, A. L. Moore, T. A. Moore, D. Gust, G. Harris, S. M. Lindsay, *Science* **2001**, *294*, 571-574.

[29] M. Hegner, P. Wagner, G. Semenza, *Surf. Sci*. **1993**, *291*, 39-46.

[30] a) L. A. Bumm, J. J. Arnold, M. T. Cygan, T. D. Dunbar, T. P. Burgin, L. Jones II, D. L. Allara, J. M. Tour, P. S. Weiss, *Science* **1996**, *271*, 1705-1707; b) G. E. Poirier, *Chem. Rev*. **1997**, *97*, 1117–1127; c) L. Patrone, S. Palacin, J. P. Bourgoin, *Appl. Surf. Sci*. **2003**, *212-213*, 446–451; d) K. Moth-Poulsen, L. Patrone, N. Stuhr-Hansen, J. B. Christensen, J.-B. Bourgoin, T. Bjørnholm, *Nano Lett*. **2005**, *5*, 783-785; e) S. Yasuda, T. Nakamura, M. Matsumoto, H. Shigekawa, *J. Am. Chem. Soc*. **2003**, *125* 16430-16433; f) Z. J. Donhauser, B. A. Mantooth, K. F. Kelly, L. A. Bumm, J. D. Monnell, J. J. Stapleton, D. W. Price, A. M. Rawlett, D. L. Allara, J. M. Tour, P. S. Weiss, *Science* **2001,** *292*, 2303-2307; g) Z. J. Donhauser, B. A. Mantooth, T. P. Pearl, K. F. Kelly, S. U. Nanayakkara, P. S. Weiss, *Japan. J. Appl. Phys*. **2002**, *41*, 4871-4877; h) P. A. Lewis, C. E. Inman, Y. Yao, J. M. Tour, J. E. Hutchison, P. S. Weiss, *J. Am. Chem. Soc*. **2004**, *126*, 12214-12215; i) G. K. Ramachandran, T. J. Hopson, A. M. Rawlett, L. A. Nagahara, A. Primak, S. M. Lindsay, *Science* **2003**, *300*, 1413-1416; j) R. A. Wassel, R. R. Fuierer, N. Kim, C. B. Gorman, *Nano Lett*. **2003**, *3*, 1617-1621; k) A. S. Blum, J. G. Kushmerik, D. P. Long, C. H. Patterson, J. C. Yang, J. C. Henderson, Y. Yao, J. M. Tour, R. Shashidhar, B. R. Ratna, *Nat. Mater*. **2005**, *4*, 167-172.

[31] W. R. Browne, J. J. D. de Jong, T. Kudernac, M. Walko, L. N. Lucas, K. Uchida, J. H. van Esch, B. L. Feringa, *Chem. Eur. J*. **2005**, *11*, 6414-6429; W. R. Browne, J. J. D. de Jong, T. Kudernac, M. Walko, L. N. Lucas, K. Uchida, J. H. van Esch, B. L. Feringa, *Chem. Eur. J*. **2005**, *11*, 6430-6441; J. Areephong, W. R. Browne, N. Katsonis, B. L. Feringa, *Chem. Commun.*, **2006**, 3930-3932.

[32] T. Tsujioka, H. Kondo, *Appl. Phys. Lett*. **2003**, *83*, 937-941.

[33] D. Dulic, S. J. van der Molen, T. Kudernac, H. T. Jonkman, J. J. D. de Jong, T. N. Bowden, J. van Esch, B. L. Feringa, B. J. van Wees, *Phys. Rev. Lett*. **2003**, *91*, 207402.

[34] L. A. Bumm, J. J. Arnold, T. D. Dunbar, D. L. Allara, P. S. Weiss, *J. Phys. Chem. B* **1999**, *103*, 8122-8127.

[35] J. Ern, A. Bens, H. D. Martin, S. Mukamel, D. Schmid, S. Tretiak, E. Tsiper, C. Kryschi, *J. Lumin*. **2000**, *742*, 87–89; J. Ern, A. Bens, H. D. Martin, S. Mukamel, D. Schmid, S. Tretiak, E. Tsiper, C. Kryschi, *Chem. Phys*. **1999**, *246*, 115-125.

[36] Note that the foregoing considerations on the Koopmans theorem justify plotting molecular energy states and the gold Fermi level together (see experimental section: "Details on Semiempirical Calculations").

[37] Calculations were performed by Dr. H. T. Jonkman.

[38] J. Li, G. Speyer, O. F. Sankey, *Phys. Rev. Lett*. **2004**, *93*, 248302.

[39] M. Zhuang, M. Ernzerhof, *Phys. Rev. B: Condens. Matter Mater. Phys*. **2005**, *72*, 073104.

[40] J. M. van Ruitenbeek, A. Alvarez, I. Piñeyro, C. Grahmann, P. Joyez, M. H. Devoret, D. Esteve, C. Urbina, *Rev. Sci. Instrum*. **1996**, *67*, 108-111.

[41] J.G. Simmons, *J. Appl. Phys*. **1963**, *34*, 1793-1803.

[42] R. Stratton, *J. Phys. Chem. Solids* **1962**, *23*, 1177-1190.

[43] J. V. Barth, H. Brune, G. Gertl, *Phys Rev B* **1990**, *42*, 9307-9318.